Identification potential sources of marine debris based on backward trajectory modelling in Tidung Island

Mochamad Dwianto[1*], *Mochamad Tri* Hartanto[1], *Erwin* Maulana[1], and *Teguh* Nugraha[1]

[1]Department of Marine Science and Technology, Faculty Fisheries and Marine Science, IPB University, Bogor 16680, Indonesia

Abstract. Marine debris poses an increasing threat to the coastal ecosystems of the Seribu Islands, particularly Tidung Island, where hydrodynamic influences on debris transport remain poorly understood. This study simulated the movement and seasonal origin of floating debris using backward modeling integrated with validated hydrodynamic and Lagrangian modules in OpenFlows FLOOD. The model, forced by tidal, wind, and bathymetric data, showed strong agreement with the field observations, with correlation coefficients of 0.84–0.94, and RMSE values of 0.069–0.097 across tidal elevation and currents. Simulations under contrasting monsoon conditions revealed current velocities of 0.10–0.28 m/s during the west monsoon and 0.03–0.24 m/s during the east monsoon, producing southwestward flow in the west season and weaker northwestward circulation in the east. Backward analysis showed that during the western monsoon, offshore debris from the northern Java Sea was advected southward and accumulated near Tidung Island, whereas during the east monsoon, debris mainly originated from local activities and remained confined due to weak circulation. These findings highlight the dual role of Tidung Island as both a receiver of offshore debris and a trap for local waste, underscoring the need for stronger community management and integrated policy actions to reduce marine debris.

Keywords: Backward modeling, marine debris, Tidung Island

1 Introduction

Marine debris have become a global environmental challenge that threatens marine ecosystems and coastal sustainability. They consist primarily of plastic materials that are resistant to degradation, allowing them to persist for long periods in marine environments. This debris causes physical harm to marine organisms through entanglement and ingestion, degrades coral habitats, and diminishes the aesthetic and economic value of tourism and fisheries [1, 2]. In Indonesia, which ranks among the largest contributors to marine plastic

* Corresponding author: mochamaddwianto@gmail.com

© The Authors, published by EDP Sciences. This is an open access article distributed under the terms of the Creative Commons Attribution License 4.0 (https://creativecommons.org/licenses/by/4.0/).

leakage worldwide, an estimated hundreds of thousands of tons of waste enter the ocean annually. This issue is particularly concerning in coastal metropolitan areas, such as Jakarta Bay and the Seribu Islands, where high population density and inadequate waste management intensify debris accumulation in the surrounding waters.

Recent research in Indonesia has revealed that marine debris around the Seribu Islands is dominated by low-density plastics originating from both local and external sources [3, 4]. Field observations in islands such as Pari, Pramuka, and Tidung have reported increasing debris accumulation driven by monsoonal circulation and limited flushing efficiency in shallow reef systems. However, most of these studies have focused on quantifying the abundance and composition of debris, with limited attention paid to the dynamic processes that govern its transport and retention. Consequently, the spatial connectivity and potential origin of debris within the Seribu Islands remains poorly understood.

Small tropical islands are highly vulnerable to marine debris, which threatens ecosystems, fisheries, and tourism sectors [5, 6]. Hydrodynamic drivers such as tides, monsoonal winds, and regional currents [7, 8]. Identifying the source of debris is therefore essential for distinguishing between local inputs and external contributions, supporting more effective management interventions [9]. The Tidung Islands, located in the southern part of the Seribu Islands in the Java Sea, exemplify a small island system where shallow bathymetry, reef-bounded channels, and seasonal monsoon influence create complex circulation and debris retention zones [10]. Circulation around the islands is primarily driven by semi-diurnal tides and monsoonal variability, with regional currents interacting with the reef flats and narrow channels. These mechanisms control the water residence time, flushing efficiency, and retention or release of suspended and floating materials, including marine debris.

To reconstructing debris pathways and assessing their potential origins, backward trajectory modelling provides a robust tool by integrating hydrodynamic forcing with field observations. In this study, the OpenFlows FLOOD platform was applied to simulate tidal and wind-driven circulation and backtrack the transport of floating debris [11]. The outcomes are expected to generate a scientific basis for targeted debris management and conservation strategies, enhancing the resilience of small tropical islands, such as Tidung, under both climatic and anthropogenic pressures.

Several studies on marine debris on the Seribu Islands have primarily focused on quantifying their abundance and composition [12, 13]. However, discussions of the physical mechanisms that control debris transport and accumulation remain limited. In reality, the interactions between monsoonal circulation, tidal oscillations, and local geomorphology play a crucial role in regulating the retention and dispersal of floating materials; however, these processes have not been sufficiently investigated in small-island environments such as Tidung. The contrasting characteristics of the west and east monsoons, each with distinct wind directions and current structures, are expected to alter the connectivity between the offshore and nearshore debris sources. To address this knowledge gap, the present study integrates hydrodynamic modeling with backward Lagrangian trajectory simulations to determine potential debris origins and understand how physical forcing governs their spatial distribution around Tidung Island.

2 Materials and method

2.1 Study area

Tidung Island, located approximately 48 km north of Jakarta, is one of the inhabited islands in the southern Thousand Islands Administrative Regency. It consists of two main parts, Tidung Besar and Tidung Kecil, connected by a wooden bridge known as Jembatan Cinta

with a combined land area of approximately 109 ha and a population exceeding 5,000 residents. The local economy is supported mainly by small-scale fisheries and marine tourism. This study was conducted in the ITK IPB Oceanography Laboratory between July and September 2025 using backward hydrodynamic and Lagrangian simulations that represent two contrasting monsoonal conditions: the west monsoon (January 2022) and the east monsoon (August 2022). The computational domain covered the southern part of the Thousand Islands, extending between 5°25′–6°10′ S and 106°2′–107°10′ E, with a specific focus on the Tidung Island region. Field measurements of tides and currents were carried out at 5.805221° S and 106.521794° E, at a depth of 3 m, over four days and three nights from March 24 to 29, 2022. The research and measurement stations are shown in **Fig. 1**.

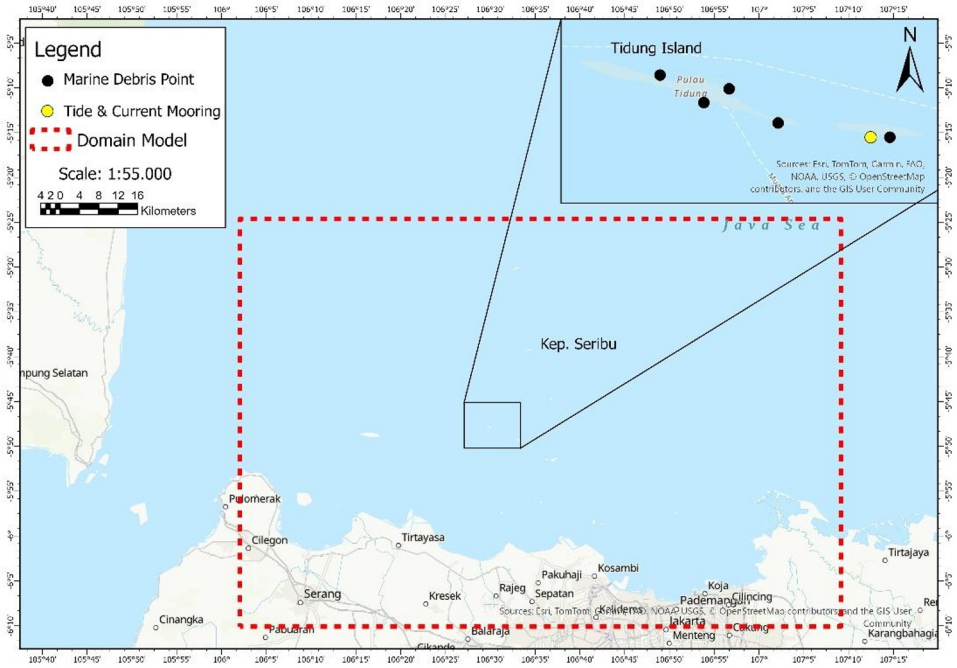

Fig. 1. Map of the research area.

The model used in this study was developed based on field observations conducted during the practicum at the Department of Marine Science and Technology, IPB University. During the survey, a significant accumulation of plastic debris was recorded along the shoreline, particularly near Jembatan Cinta and the western part of Tidung Besar. The debris was dominated by floating low density polyethylene (LDPE) materials such as plastic bags and food wrappers, with an average density of approximately 0.9 g/cm³, which allows them to remain buoyant and be transported by surface currents. Based on the field survey, five monitoring points were designated as debris observation sites, with three around Tidung Besar, one at Jembatan Cinta, and one at Tidung Kecil representing identified hotspots of debris accumulation.

2.2 Data sources

The data used in this study consisted of field observation data, including tidal elevation, which served as the basis for model validation. In addition, reanalysis datasets comprising tidal, bathymetry, and wind data were used as inputs for the model configuration (**Table 1**).

Tidal and current measurements were conducted using the Eulerian method through mooring, with tidal records taken at one-minute intervals, and current records taken at 30 second interval, were recorded continuously over a period of four days and three nights. These observational data were used to validate the outputs of the hydrodynamic model [14].

Bathymetric data were obtained from the Indonesian National Bathymetry (BATNAS), with a spatial resolution of 15 arcseconds, approximately 30 m. Wind data were sourced from the Copernicus Marine Environment Monitoring Service (CMEMS) with a temporal resolution of six hours [15]. Tidal data were also obtained from the Finite Element Solution (FES) 2014 tidal model developed by Laboratoire d'Etudes en Geophysique et Oceanographie Spatiales (LEGOS), which was used as a boundary input for the hydrodynamic model setup.

Table 1. Sources and resolutions of data used in the study.

Data	Data Acquisition		Resolutions	Sources
	Observation	Reanalysis		
Tide Elevation (Validation)	√		Mooring data in 4 days and 3 night, interval 1 minute (3-24-2022 until 03-29-2022)	Observation Tide Logger JFE Compact TD
Current Direction & Velocity	√		Mooring data in 4 days and 3 night, interval 30 second (3-24-2022 until 03-29-2022)	Observation Current meter JFE Infinity EM
Tide Prediction (Input Model)		√	resolution grid 1/16°	FES2014 (Aviso Altimetry)
Bathymetry		√	resolution grid 15-arc second	Batimetri Nasional (BATNAS) 2024
Wind Direction and Speed		√	grid resolution 0,15 degree, interval 6 hour	Copernicus Marine Service (https://marine.copernicus.eu/)

2.3 Hydrodynamic modeling

The simulation was conducted using OpenFlow Flood, which employs a finite-volume scheme as its numerical foundation [16, 17]. This scheme, based on flux-conserving computations, allows multiple physical processes to be solved simultaneously, and is implemented using ANSI FORTRAN 95. The model utilized a single-layer vertical geometry with a temporal resolution of 60 s per time step, totaling 20,160 time steps, equivalent to a 15-day simulation period. Bathymetric data were obtained from BATNAS 2024, tidal forcing was obtained from the FES2014 tidal atlas [18], and atmospheric forcing was obtained from the Copernicus Marine Service. The open boundary facing the Java Sea applies tidal elevation and wind forcing, while the closed boundaries along Jakarta Bay and the surrounding islands restrict landward flow [19]. The computational domain was constructed using a nested grid system to represent both large-scale dynamics and local circulation, consisting of three grid resolutions, 1000 m (blue), 500 m (green), and 100 m (red). The model domain and grid system are illustrated in **Fig. 2**.

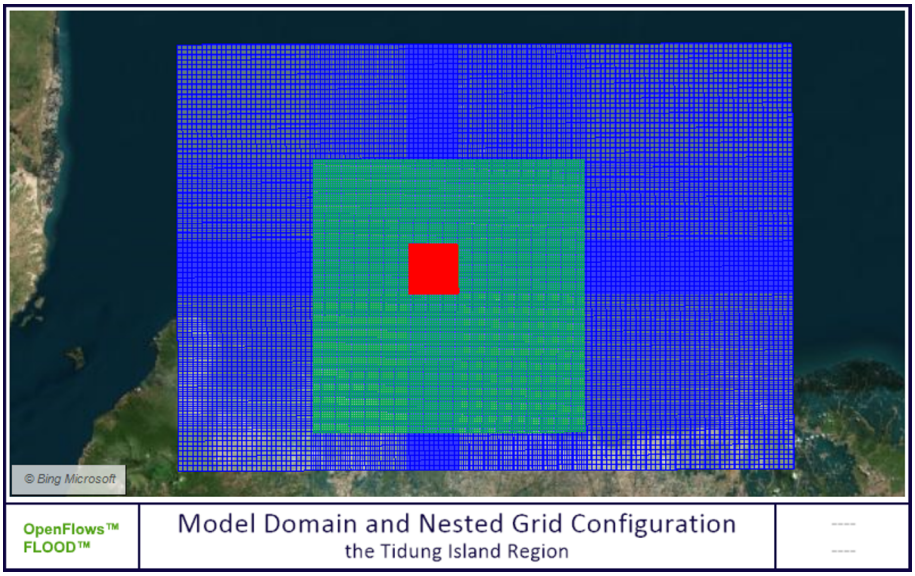

Fig. 2. Model domain and nested grid configuration.

The Lagrangian particle-tracking module was coupled with a hydrodynamic simulation to model the movement of floating debris influenced by surface currents and wind. This module computes particle trajectories based on the velocity fields derived from the hydrodynamic results. A total of 100 virtual particles were released, representing low density polyethylene (LDPE) plastics with a density of 0.9 g/cm³, allowing them to remain buoyant and be transported by surface currents. The simulation was conducted in backward mode for a 15-day period to trace potential debris source areas, with particle positions recorded hourly to analyze transport pathways and connectivity between Tidung Island and its surrounding waters. A summary of the model configurations and boundary conditions is provided in **Table 2**.

Table 2. Configuration of the hydrodynamic model.

Parameter		Value	Unit	Notes
Grid 1	Cell Numbers X (I)	100	Cell	
	Cell Numbers Y (J)	100	Cell	
	Grid Size	100	m	
Grid 2	Cell Numbers X (I)	110	Cell	
	Cell Numbers Y (J)	110	Cell	
	Grid Size	500	m	
Grid 3	Cell Numbers X (I)	86	Cell	
	Cell Numbers Y (J)	125	Cell	
	Grid Size	1000	m	
Number of time step		20.160	-	
Time step interval		60	second	
Geometry		1	layers	
Tide		1/8	degree	Fes 2014
Bathymetry			m	Batnas 2024
Atmosphere	Wind		m/s	Copernicus Marine Service
Boundaries	Open Boundaries			Tide and Wind
	Close Boundaries			Coastline of Jakarta Bay and Islands around

In this simulation model, a Lagrangian module with a single-layer geometry was applied. The particles used in this study represent LDPE (Low-Density Polyethylene) plastic, which has a density of 0.9 g/cm³. This type of plastic, commonly found as residues of anthropogenic activities in coastal areas such as plastic bags and food wrappers, tends to float on the ocean surface and is easily transported by hydrodynamic forces.

The total number of particles released was 20 per station, and five monitoring points were established to observe marine debris: three located around Tidung Besar Island, one on Jembatan Cinta, and one on Tidung Kecil Island. These observation points were determined based on field surveys conducted by Marine Science and Technology students from IPB University during a field practicum on Tidung Island, where debris accumulation hotspots were identified.

2.4 Model validation

Assessing the reliability of hydrodynamic simulations is critical for ensuring that the model outputs accurately represent real-world conditions. In this study, model validation was performed using two comparative approaches, and the model was validated by comparing tidal simulation results based on boundary input from FES2014 with sea-level data obtained from field measurements. Current velocity simulations were validated using data collected directly at the study site through field observations. Several statistical metrics were employed to quantitatively measure the agreement between the model and observations. The Root Mean Square Error (RMSE) served as the primary indicator quantifying the average magnitude of deviation between the simulated and observed values. RMSE is widely recognized as a standard performance metric across environmental modeling disciplines, including climate, meteorology, and oceanography [20]. The RMSE formulation applied in this study is shown in Equation 5.

$$RMSE = \sqrt{\frac{1}{n}\sum_{i=1}^{i}(y - y')^2} \quad (1)$$

Complementing the RMSE analysis, two additional metrics were calculated: the standard deviation, which describes the dispersion of data values relative to the mean, and the Pearson correlation coefficient (R), which reflects the temporal agreement and consistency of data trends between the model and field observations. Together, these metrics offer a more comprehensive understanding of the model fidelity, capturing both the error magnitude and dynamic behavior of the system. To further enhance the interpretation, the results were visualized using a Taylor Diagram, a widely used graphical tool in geophysical sciences for assessing model skill. This diagram integrates RMSE, standard deviation, and correlation into a single 2D plot, providing an intuitive representation of how well the model replicates the observed phenomena [21]. The diagram was produced in JupyterLab within the Anaconda 3 environment, which supports robust data visualization and scientific computing. To interpret the RMSE values, this study adopted the classification system proposed by [22], which defines the performance categories, as shown in **Table 3**.

Table 3. RMSE performance classification.

Model Performance Category	RMSE Value Range
Very Good	RMSE ≤ 0.5
Good	0.5 < RMSE ≤ 0.6
Moderate	0.6 < RMSE ≤ 0.7
Poor	RMSE > 0.7

3 Results and discussions

3.1 Validation of tide and current between observation and model result

The accuracy of the tidal and current data from the U and V simulations was assessed by comparing model outputs with field observations of the water level. Statistical evaluation was conducted using the correlation coefficient, root mean square error (RMSE), and standard deviation, and the results are illustrated in the Taylor diagram (**Fig. 3**).

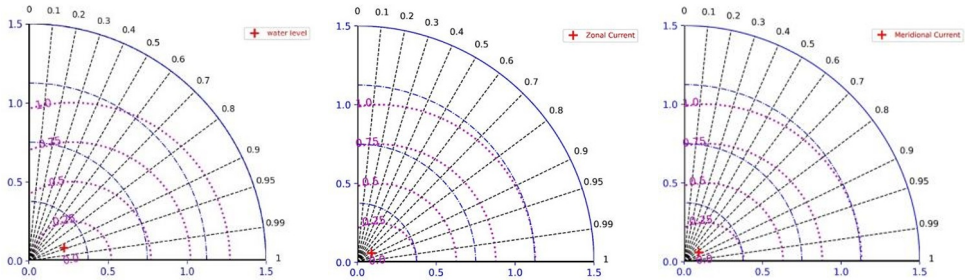

(A) Water level (B) Zonal Current (C) Meridional Current

Fig. 3. Taylor diagram for tidal validation, in March 2022.

The hydrodynamic model validation against observed tidal elevation (**Fig. 3A**) shows a strong agreement, with a correlation coefficient of 0.94, RMSE of 0.097 m, and standard deviations of 0.27 m (observed) and 0.24 m (modeled), indicating a minimal bias in tidal variability. Consistent performance was also observed in the current validation: the zonal current (U) component (**Fig. 3B**) achieved a correlation of 0.84 and RMSE of 0.0699 m/s, with standard deviations of 0.127 m/s (observed) and 0.107 m/s (modeled), while the meridional (V) component (**Fig. 3C**) showed a correlation of 0.85, RMSE of 0.0691 m/s, and standard deviations of 0.130 m/s (observed) and 0.110 m/s (modeled). These quantitative metrics demonstrate that the model effectively reproduces both the amplitude and temporal variability of tidal and current dynamics. The proximity of all markers to the reference point in the Taylor diagrams confirms that the deviations are within acceptable thresholds for coastal hydrodynamic applications. Therefore, the model can be considered valid and robust, providing a reliable foundation for subsequent simulations of the current circulation and debris transport around Tidung Island. A comparison between the simulated and observed tidal elevations is shown in **Fig. 4**, and a comparison of the current velocity is shown in **Fig. 5**.

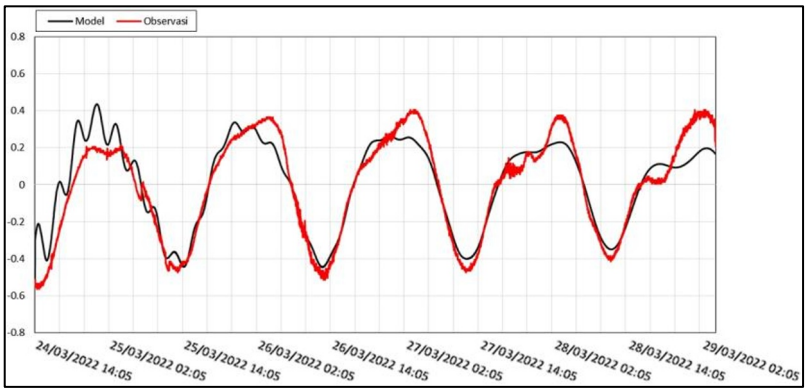

Fig. 4. Validation of the modeled water level elevation against field measurement data.

The model (black line) closely followed the observed water level (red line), successfully capturing both the phase and amplitude of the tidal cycles throughout the simulation period from March 24 to 29, 2022. Minor discrepancies are evident at certain peak and trough events, where the model slightly underestimates the maximum tidal elevations; however, the overall agreement remains strong. This visual consistency reinforces the statistical findings, confirming that the model provides a realistic representation of the tidal dynamics at Tidung Island, and can be confidently applied as the basis for subsequent hydrodynamic and particle transport simulations. Although the validation was conducted using observational data from March 2022, the results demonstrate that the model is sufficiently reliable for reproducing the tidal dynamics in the study area. Based on this validation, the model can be applied to simulate different seasonal conditions, including the west monsoon in January and the east monsoon in August 2022. This approach ensures that the model setup is grounded in field observations while also enabling broader applications for assessing hydrodynamic variability across different monsoonal periods around Tidung Island.

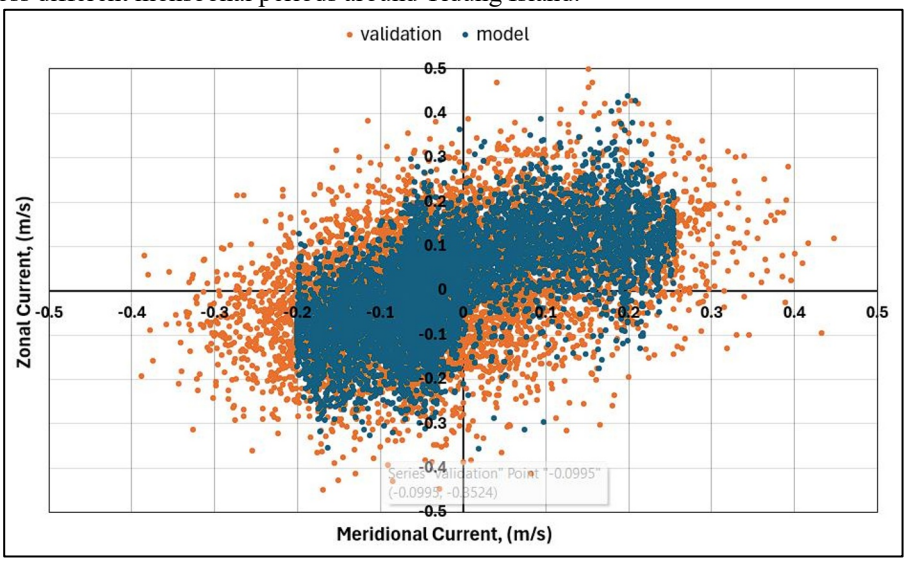

Fig. 5. Scatter plot of observed and simulated currents at Tidung Island.

The scatter diagram shows that the current pattern around Tidung Island is mainly controlled by tidal motion, resulting in back-and-forth flow. Two datasets are shown; the blue points represent the model results, while the orange points represent field observations, and their close overlap indicates that both capture a similar current pattern. The data are distributed symmetrically around the zero axis for both the zonal (U) and meridional (V) components, showing that the current moves alternately eastward–westward and northward–southward with almost equal strength. The U component reaches about +0.4 m/s eastward and –0.4 m/s westward, while the V component varies between +0.5 m/s northward and –0.5 m/s southward. The elliptical spread of points across all quadrants indicates periodic current reversals, during which the flow tends to move northeastward (U+ and V+), and during the ebb tide, it turns southwestward (U– and V–). This alternating pattern reflects the typical tidal circulation in the shallow waters of the Seribu Islands, where semidiurnal tides drive the current to regularly change direction. With maximum speeds of 0.4–0.5 m/s, the current can be classified as moderate and is capable of moving fine sediments and floating materials in rhythm with the tidal cycle. Although validated using March 2022 data, the steady physical setup of the model allows reliable simulation of the January and August 2022 monsoon conditions.

3.2 Current patterns in the west and east monsoon

During the western monsoon period, the atmospheric system over western Indonesia was dominated by monsoons. During the west monsoon, prevailing westerlies to northwesterlies drive the surface flow eastward to northeastward across the Java Sea [23]. These winds cross the eastern Indian Ocean and Java Sea, driving the surface water masses from west to east. On a regional scale, this pattern causes surface currents in the northern Java Sea to flow eastward or northeastward following the wind direction [24]. However, when this flow approaches the Seribu Islands region, its direction begins to change owing to the influence of the complex local bathymetry and coastal topography [25].

The Seribu Islands form a chain of shallow islands and coral reefs extending from north to south separated by narrow passages [26]. When the eastward flow from the northern Java Sea enters this area, it no longer moves directly with the wind direction, but experiences deflection and channeling. The combination of shallow depth, coral shoals, and numerous small islands forces the flow to follow seabed contours. Some of the incoming currents from the north and northeast are redirected through the inter-island passages toward the south and southwest, whereas the flow along the outer shelf forms weak eddies in the lee of larger islands. As a result, the surface current around Tidung Island shows a southwestward tendency in contrast to the eastward regional current of the open Java Sea.

In addition to topographic steering, circulation is influenced by inflow from the Sunda Strait. During the western monsoon, the sea level in the eastern Indian Ocean is slightly higher than that in the Java Sea, generating a weak pressure gradient that drives water into the southern part of the Seribu Islands [27]. The interaction between this inflow and the northern Java Sea current creates a complex pattern in the southern archipelago, often resulting in current deflection and localized stagnation zones around Tidung Island.

Hydrodynamic simulation indicated that the current speeds varied with the tidal phase (**Fig. 6**). During the toward-ebb phase (**Fig. 6A**), currents begin to strengthen westward along the northwestern boundary, with velocities ranging from 0.10 to 0.20 m/s, while around Tidung Island and within passages they remain below 0.10 m/s. At the peak of ebb (**Fig. 6B**), the strongest flow occurs near the northwestern offshore zone, reaching a maximum of 0.28 m/s, forming a dominant westward jet, while inter-island passages record 0.05–0.10 m/s. During the toward-flood phase (**Fig. 6C**), currents rotate and weaken to 0.10–0.15 m/s offshore and below 0.10 m/s near the islands. At the peak of the flood (**Fig. 6D**), the flow intensified again in the northern sector to approximately 0.20–0.25 m/s, while inside passages it remained weak, accompanied by small recirculating eddies. These variations indicate that tidal oscillations primarily modulate the current intensity without reversing the general southwestward direction, with ebb currents remaining slightly stronger and more organized than flood currents.

The combined influence of western monsoon winds, inflow from the Sunda Strait, and complex island topography produces a distinct southwestward circulation that channels surface water from the northern Java Sea toward the central and southern Seribu Islands. This hydrodynamic condition explains the gradual advection of floating materials toward Tidung Island. This result is consistent with backward simulations showing that during the West Monsoon, debris originating from offshore waters in the northern Java Sea was transported southward and trapped around Tidung Island because of residual flow, tidal oscillation, and topographic steering.

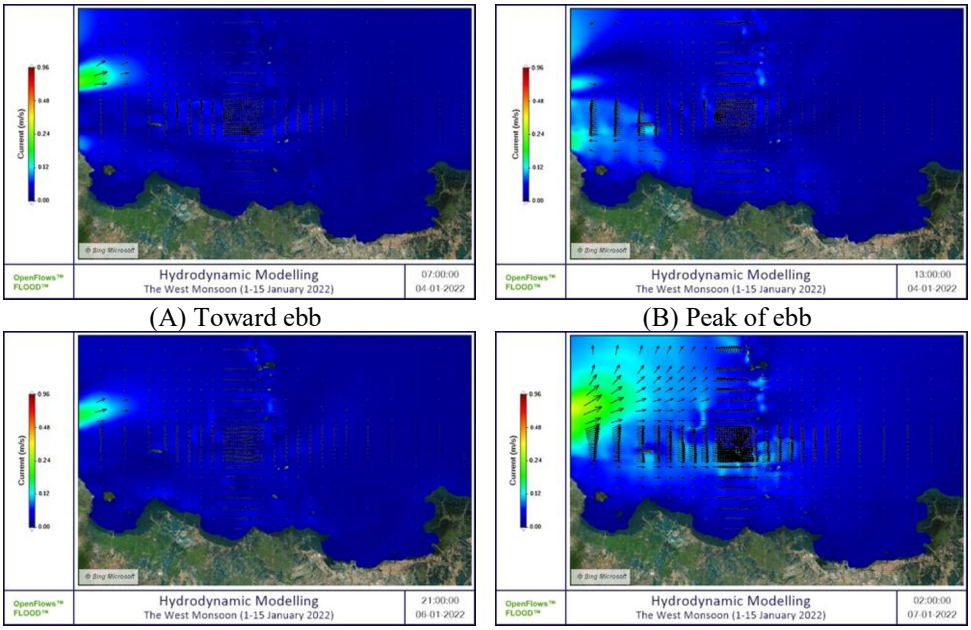

Fig. 6. Hydrodynamic modelling at the west monsoon (1-15 January 2022).

Hydrodynamic modeling for the eastern monsoon period reveals circulation patterns opposite to those observed during the western monsoon. During this season, southeast winds prevail and drive the surface water northwestward across the northern Java Sea. When these currents enter the Seribu Islands region, particularly near Tidung Island, their direction and magnitude vary because of the influence of island configuration and shallow bathymetry [28]. In general, current speeds in the open Java Sea range from 0.10–0.20 m/s, while within inter-island passages they decrease to 0.03–0.10 m/s. The highest velocities occur in the northern part of the Seribu Islands facing the open sea, whereas the lowest values appear in the central and southern sectors, where bottom friction and coral reef structures reduce flow energy [29].

During the toward-ebb phase (**Fig. 7A**), the flow moves weakly northwestward at 0.05–0.10 m/s offshore and below 0.05 m/s near Tidung Island. At the peak of ebb (**Fig. 7B**), northern currents intensify to 0.20–0.24 m/s with a clear northwestward orientation, reflecting the persistent southeast monsoon winds. Within the passages, the flow weakened and formed local recirculating motions between the reefs. During the toward-flood phase (**Fig. 7C**), the current slows and begins to shift southeastward at 0.05–0.10 m/s, indicating stronger tidal influence. At the peak of flood (**Fig. 7D**), the flow strengthens slightly in the outer waters, reaching around 0.24 m/s, while within the central archipelago it remains below 0.10 m/s.

Overall, the east monsoon circulation is calmer and more stable than that of the western monsoon. The dominant northwestward flow in the open sea weakens within the archipelago, forming semi-enclosed circulation cells with a low flushing efficiency. This hydrodynamic condition promotes water retention and localized stagnation zones near Tidung Island. The backward model results align with this finding, showing that during the east monsoon, most floating particles remain confined within the Seribu Islands rather than originating from offshore, suggesting that debris accumulation around Tidung Island primarily results from local activities, such as tourism, small-scale fisheries, and domestic waste sources [30].

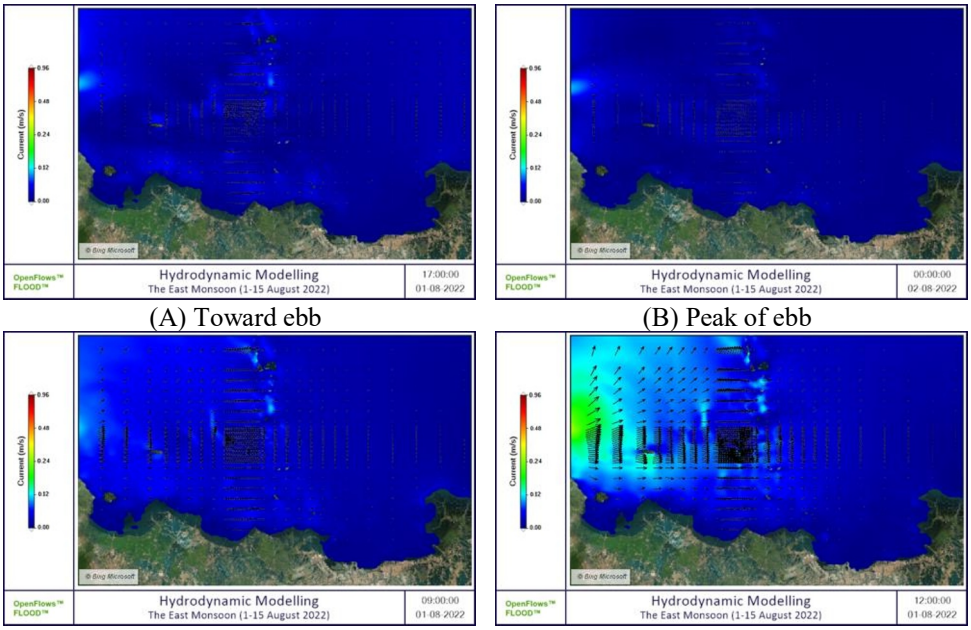

(A) Toward ebb (B) Peak of ebb

(C) Toward flood (D) Peak of flood

Fig. 7. Hydrodynamic modelling at the east monsoon (1-15 August 2022).

3.3 Seasonal backward of debris trajectories

The backward simulation for the west monsoon period (January 1–15, 2022) traces the trajectory of floating plastic debris at the sea surface as it migrates across the Java Sea and Seribu Islands region before finally accumulating around Tidung Island. In this inverse modeling approach, day 15 represents the earliest origin point of plastics offshore, whereas day 1 shows their final concentration near Tidung. Given the strong validation performance for tidal dynamics ($r = 0.94$, RMSE = 0.097 m) and the known forcing of strong east–northeast monsoon winds, the results provide robust insights into the transport pathways of debris. Similar approaches have been applied in regional and global studies that highlight the importance of seasonal monsoon forcing in shaping plastic dispersal [31].

On day 15, debris was widely scattered across the open waters of the Java Sea to the north and northwest of the Seribu Islands, reflecting an external origin outside the local archipelago. The persistent east–northeast winds of the west monsoon drive residual surface currents westward, gradually advecting debris toward the island chain. Although diurnal tides impose daily oscillatory motion, they do not override the prevailing westward drift. This pattern is consistent with earlier modeling work in Indonesian waters, which showed that offshore plastics can be transported into archipelagic corridors under monsoon forcing [32]. By days 12 and 9, the particles moved progressively southward, entering the northern and central sectors of the Seribu Islands. Their spread narrows as they are funneled between islands, illustrating the role of monsoon-driven currents in channeling plastics offshore toward more confined straits.

On day 6, the debris field became denser in the western waters near Tidung Island, marking a transitional stage where offshore plastics began mixing with potential local sources. The diurnal tide still generates oscillations, yet the dominant pathway remains north–south advection. By day 3, trajectories indicated proximity to the western Java coastline and western Seribu Islands, suggesting that part of the debris stream may be associated with land-

based sources such as river outflows or coastal leakage. This interpretation aligns with evidence that Jakarta Bay and its river systems are among the largest contributors to plastic leakage to the sea in Indonesia [33]. Finally, on day 1, all trajectories converged at Tidung Island, where plastics accumulated. The backward reveals a clear storyline, plastics floating offshore in the Java Sea are captured by monsoon-driven currents, oscillate under tidal forcing, move gradually southward through the island chain, and ultimately strand around Tidung. This sequence echoes the finding that positively buoyant plastics can travel long distances across regional seas before accumulating in small-island ecosystems. The model for the western monsoon is shown in **Fig. 8**.

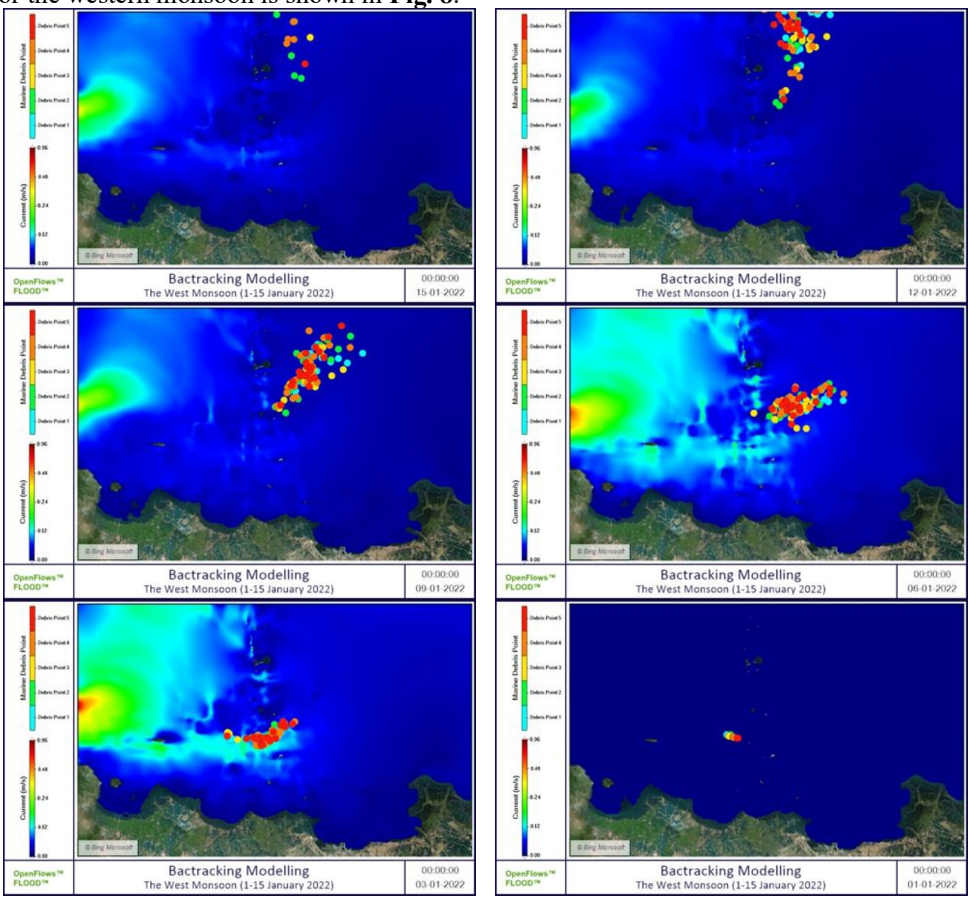

Fig. 8. Backward modelling at the west monsoon (1-15 January 2022).

The backward simulation for the east monsoon period (August 1–15, 2022) revealed a markedly different trajectory of floating plastic debris compared to the west monsoon scenario (**Fig. 9**). During this season, the prevailing winds blow from the west–southwest at slow to moderate intensities (0.2–2.4 m/s), creating surface currents directed eastward, but with weaker flushing efficiency than in January. Such circulation conditions extend the residence time of plastics within the Seribu Islands, allowing debris released from local human activities to remain trapped in the nearshore zones for longer periods.

At the beginning of the backward sequence (day 15), the modeled particles were already situated close to the southern and central sections of the Seribu Islands, suggesting that localized sources played a stronger role than offshore inputs. Unlike the dispersive patterns evident in January, the August trajectories showed a limited spread into the open Java Sea.

This behavior is consistent with weaker wind stress during the east monsoon, which reduces the capacity of currents to transport plastics across wider areas [34].

By days 12 and 9, clusters of debris appeared between Tidung Island and its adjacent islands, exhibiting only a gradual displacement under the influence of diurnal tidal oscillations. The absence of long offshore excursions indicates that the debris predominantly originated from anthropogenic sources within the island group itself, such as coastal settlements, artisanal fisheries, and tourism operations, all of which are known contributors to nearshore marine debris in the Indonesian archipelago. As the sequence progressed to day 6, the debris field became denser and revealed convergence zones in the central Seribu Islands, where weak circulation allowed the debris to linger. Under such conditions, plastics that would otherwise disperse are re-entrained by local eddies or tidal pumping. Similar processes have been observed in reef-dominated systems in Southeast Asia, where calmer seasonal conditions enhance pollutant retention and increase local ecological vulnerability.

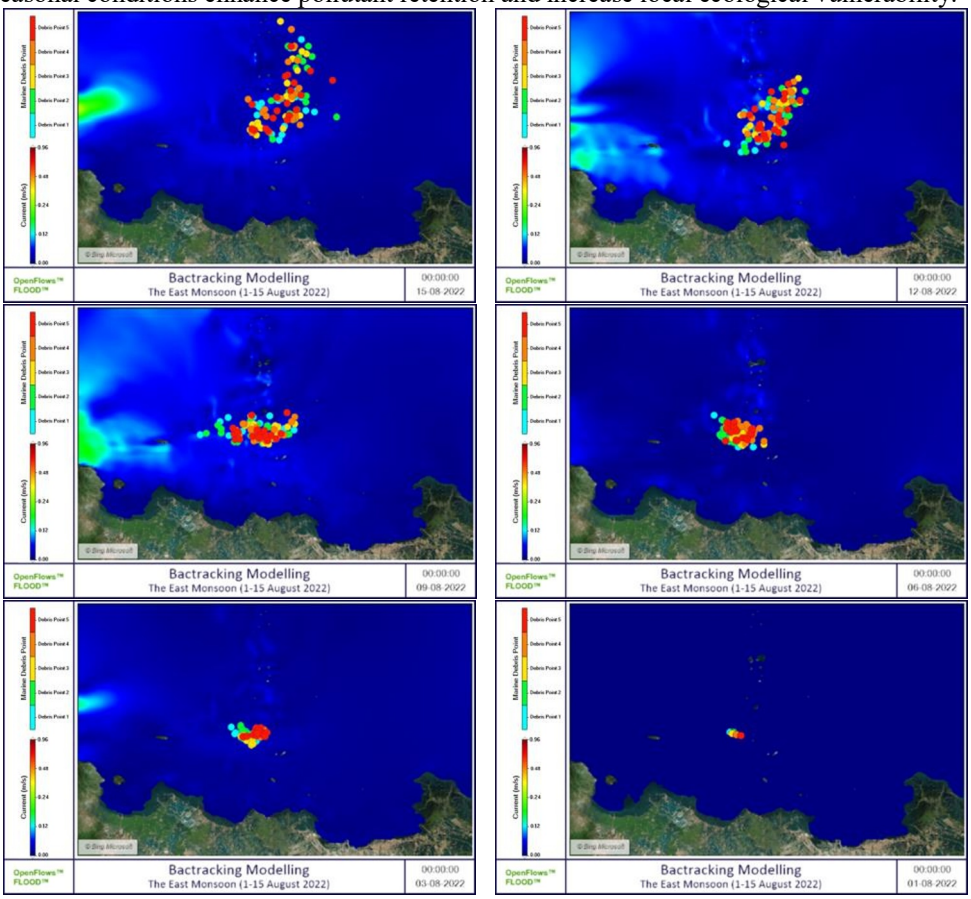

Fig. 9. Backward modelling at the east monsoon (1-15 August 2022).

By day 3, the trajectories continued to concentrate around Tidung Island and nearby reefs, with only minor dispersal toward the western Java coastal waters. This strongly supports the interpretation that under east monsoon conditions, external inputs from the Java Sea are minimal, and the accumulation signal is dominated by local recirculation. The reduced advective strength of currents and prolonged water residence time create an environment in which plastics can persist for extended durations without being flushed away.

Finally, by day 1, all trajectories converged directly on Tidung Island, marking it as the terminal sink for this circulation regime. This sequence illustrates that during the east monsoon, the plastics found in Tidung are primarily the product of localized recycling within the Seribu Islands, exacerbated by weak dispersive forces. This is in stark contrast to the west monsoon, when strong offshore currents carry debris from the open Java Sea into the island chain. Together, these findings underscore how seasonal monsoon reversals reshape the connectivity between offshore and island waters, shifting Tidung Island from being a receptor of external inputs in January to a trap of locally generated debris in August.

Backward simulations show that seasonal dynamics strongly shape the origin and transport of floating plastics around Tidung Island. This modeled accumulation pattern is consistent with field observations of debris hotspots around the central Seribu Islands, including Tidung Island, where local waste inputs dominate. In the west monsoon, strong east–northeast winds and residual currents carry debris from offshore Java Sea sources into the Seribu Islands, underscoring the role of external inputs. In contrast, the east monsoon's weaker west–southwest winds and reduced flushing promote local retention, with plastics recirculating within the archipelago and accumulating from island-based activity. These regimes reveal Tidung Island's dual vulnerability as both a receptor of offshore debris during energetic monsoon forcing and a trap for local waste under calmer conditions.

The Seribu Islands region is not directly influenced by the main pathways of Indonesian Throughflow (ITF). The core of the ITF originates from the western Pacific Ocean and flows southward through the Makassar Strait before exiting the Indian Ocean via the Lombok, Ombai, and Timor Straits [35]. The Java Sea, including the area around Tidung Island, lies outside this primary corridor and acts as a semi-enclosed basin whose circulation is predominantly governed by local tidal oscillations and seasonal monsoon winds, rather than by throughflow advection [25]. Considering this geographical setting, the ITF was not incorporated as a forcing component in the hydrodynamic model, as its influence on circulation around the Seribu Islands is minimal at the spatial and temporal scales represented in this study. The model configuration therefore focuses on the dominant physical drivers that shape local hydrodynamics, namely monsoonal wind stress, tidal forcing, and topographic steering, which collectively control current variability and water transport within the Java Sea and Seribu Islands.

4 Conclusion

This study successfully simulated the movement and seasonal origin of marine debris stranded along the coast of Tidung Island using backward modeling integrated with hydrodynamic and Lagrangian modules. The model showed strong agreement with field observations, with correlation coefficients ranging from 0.84 to 0.94 and RMSE values between 0.069 and 0.097 across tidal elevation, zonal (U), and meridional (V) currents. These results confirm the reliability of the model in reproducing local hydrodynamics. During the west monsoon, current velocities ranged from 0.10 to 0.28 m/s with a prevailing southwestward flow shaped by westerly winds and inflow from the Sunda Strait, while during the east monsoon, weaker currents of 0.03 to 0.24 m/s moved northwestward under calmer southeast winds and the influence of shallow reef topography. These seasonal contrasts generated a more dynamic circulation during the western monsoon and a semi-enclosed, low-flushing system during the eastern monsoon.

Backward analysis revealed that in the west monsoon, floating LDPE debris primarily originated from offshore waters of the northern Java Sea and was advected southward through the island chain before accumulating near Tidung Island. In contrast, during the east monsoon, debris mainly came from local human activities and remained confined within the Seribu Islands owing to weak circulation and prolonged residence time. These findings

highlight the need for coordinated and multiscale efforts to mitigate marine debris in small-island environments. At the local level, strengthening community-based waste management and circular practices can reduce inputs from tourism, fisheries, and domestic sources, whereas at higher administrative levels, integrating hydrodynamic modeling into marine debris management, enhancing waste interception in riverine systems, and reinforcing producer responsibility are essential to ensure the long-term protection of island ecosystems. Collectively, these measures can empower both communities and governing bodies to address the combined pressures of external and internal debris accumulation, which threaten the ecological and economic sustainability of Tidung Island.

References

1. R. Jambeck, R. Geyer, C. Wilcox, T.R. Siegler, M. Perryman, A. Andrady, R. Narayan, K.L. Law, Plastic waste inputs from land into the ocean. Science. **347**, 768 (2015). https://doi.org/10.1126/science.1260352
2. S.P. Manurung, H.Q. Sumardi, D.F. Lubis, M.S. Harefa, Dampak pembuangan sampah terhadap lingkungan pesisir Pantai Putra Deli: Analisis jenis sampah dominan. Studi Adm. Publik Ilmu Komun. **2**(3), 01–09 (2025).
3. P. Vriend, H. Hidayat, J. van Leeuwen, M. Cordova, N.P. Purba, A. Löhr, I. Faizal, N. Ningsih, K. Agustina, S. Husrin, D. Suryono, I. Hantoro, B. Widianarko, P. Lestari, B. Vermeulen, T. van Emmerik, Plastic pollution research in Indonesia: State of science and future research directions to reduce impacts. Front. Environ. Sci. **9**, 692907 (2021).
4. A.D. Syakti, N.V. Hidayati, R.P. Jaya, S.H. Siregar, D. Yona, F. Idris, Beach macro-litter monitoring and floating microplastic in the coastal area of Tidung Island, Indonesia. Mar. Pollut. Bull. **122**, 217 (2017). https://doi.org/10.1016/j.marpolbul.2017.06.046
5. S. Arabi, A. Nahman, Impacts of marine plastic on ecosystem services and economy: State of South African research. S. Afr. J. Sci. **116**, 5 (2020). https://doi.org/10.17159/sajs.2020/7695
6. G.G.N. Thushari, J.D.M. Senevirathna, Plastic pollution in the marine environment. Heliyon. **6**, 8 (2020). https://doi.org/10.1016/j.heliyon.2020.e04709
7. E.A. Kisnarti, N.S. Ningsih, M.R. Putri, N. Hendiarti, B. Mayer, Dispersion of surface floating plastic marine debris from Indonesian waters using hydrodynamic and trajectory models. Mar. Pollut. Bull. **198**, 115779 (2023). https://doi.org/10.1016/j.marpolbul.2023.115779
8. G. Ruffini, R. Briganti, J. Stolle, P. De Girolamo, Numerical analysis and prediction of the effect of debris initial configurations on their dispersion during extreme-hydrodynamic events. Coastal Eng. **198**, 104702 (2025). https://doi.org/10.1016/j.coastaleng.2025.104702
9. M.R. Cordova, I.S. Nurhati, Major sources and monthly variations in the release of land-derived marine debris from the Greater Jakarta area, Indonesia. Scientific Reports. **9**, 18739 (2019). https://doi.org/10.1038/s41598-019-55065-2
10. Y. Hayati, L. Adrianto, M. Krisanti, W.S. Pranowo, F. Kurniawan, Magnitudes and tourist perception of marine debris on small tourism island: Assessment of Tidung Island, Jakarta, Indonesia. Mar. Pollut. Bull. **158**, 111393 (2020). https://doi.org/10.1016/j.marpolbul.2020.111393

11. H. Ajiwibodo, M.B. Pratama, Hydrodynamic changes Impacted by the waterway capital dredging in Cikarang Bekasi Laut channel, West Java, Indonesia. Wat. Prac. & Tech. **15**, 2, 450–459 (2020). https://doi.org/10.2166/wpt.2020.032
12. N.R. Ramadhanty, Widodo, R. Suharti, H. Irawan, M. Maulita, S. Aini, A. Putra, Kristijarso, P. Arisandi, Spatial distribution of marine debris in Jakarta's Bay waters and the Seribu Islands with maritime security concept. Am. Sci. Res. J. Eng. Technol. Sci. **84**(1), 175–186 (2021).
13. K. Hutagaol, A.R. Pratama, F.A. Sirodz, P. Ramdan, A. Febriadi, T. Situmorang, The impact of environmental pollution in the Thousand Islands. Dharmwangsa Int. J. Soc. Sci. Educ. Humanit. **6**(3), 483–489 (2025).
14. T. Nugraha, I.W. Nurjaya, Rastina, S. Susanti, Characteristics of current pattern in Jakarta Bay in the west and east monsoons. J. Ilmu Teknol. Kelaut. Trop. **17**, 42–62 (2025). https://doi.org/10.29244/jitkt.v17i1.41406
15. L.H.P. Garbossa, A.A. dos Santos, K.R. Lapa, Seaweed dispersion under different environmental scenarios based on branches settling velocity and hydrodynamic Lagrangian model. Reg. Stud. Mar. Sci. **47**, 101909 (2021). https://doi.org/10.1016/j.rsma.2021.101909
16. H. de Pablo, J. Sobrinho, M. Garcia, F. Campuzano, M. Juliano, R. Neves, Validation of the 3D-MOHID hydrodynamic model for the Tagus coastal area. Water **11**, 1713 (2019). https://doi.org/10.3390/w11081713
17. H. de Pablo, J. Sobrinho, D. Garaboa-Paz, C. Fonteles, R. Neves, M.B. Gaspar, The influence of the river discharge on residence time, exposure time and integrated water fractions for the Tagus estuary Portugal. Front. Mar. Sci. **8**, 734814 (2022). https://doi.org/10.3389/fmars.2021.734814
18. X. Xu, H. Pan, F. Teng, G. Fang, Z. Wei, A comparison of global and regional ocean tide models with tide gauges in the East Asian marginal seas. J. Sea Res. **201**, 102527 (2024). https://doi.org/10.1016/j.seares.2024.102527
19. T. Chai, R.R. Draxler, Root mean square error (RMSE) or mean absolute error (MAE)? — Arguments against avoiding RMSE. Geosci. Model Dev. **7**, 1247 (2014). https://doi.org/10.5194/gmd-7-1247-2014
20. D.N. Moriasi, M.W. Gitau, N. Pai, P. Daggupati, Hydrologic and water quality models: performance measures and evaluation criteria. Transactions of the ASABE. **58**, 1763–1785 (2015). https://doi.org/10.13031/trans.58.10715
21. M.A. Ghorbani, R. Jani, F. Mohajeri, F. Daneshvar, E. Shabani, M. Khafagy, The Taylor diagram with distance: A new way to compare the performance of models. Iran. J. Sci. Technol. Trans. Civ. Eng. **49,** 2 (2024).
22. H. Khoshvaght, R.R. Permala, A. Razmjou, M. Khiadani, A critical review on selecting performance evaluation metrics for supervised machine learning models in wastewater quality prediction. J. Environ. Chem. Eng. **13**(6), 119675 (2025). https://doi.org/10.1016/j.jece.2025.119675.
23. A.S. Atmadipoera, R. Molcard, G. Madec, S. Wijffels, J. Sprintall, I. Jaya, Characteristics and variability of the Indonesian Throughflow water at the outflow straits. Deep-Sea Res. I **56**, 1942 (2009). https://doi.org/10.1016/j.dsr.2009.06.004
24. D. Sugianto, Kajian kondisi hidrodinamika (pasang surut, arus, dan gelombang) di perairan Grati Pasuruan, Jawa Timur. J. Mar. Sci. **14**, 2 (2010).
25. Y. Xu, Y. Wang, S. Hu, Y. Zhu, J. Zuo, J. Zeng, Study on the impact of the coastline changes on hydrodynamics in Xiangshan Bay. Appl. Sci. **13**(14), 8071 (2023). https://doi.org/10.3390/app13148071

26. I. Faizal, D. Iriana, I. Riyantini, N.P. Purba, The status of coral reefs in the Seribu Islands National Park Indonesia in various zones. Glob. Sci. J. **7**, 10 (2019).
27. H. Rahmawitri, A.S. Atmadipoera, S.S. Sukoraharjo, Pola sirkulasi dan variabilitas arus di perairan Selat Sunda. J. Kelautan Nas. **11**(3), 141–157 (2016).
28. R.F. Rahawarini, V. Dermawan, M.A. Sajali, Studi hidrodinamika aliran dengan model numerik DELFT3D di Pantai Sakura, Kepulauan Seribu. J. Teknol. Rekayasa Sumber Daya Air. **5**(2), 1053–1062 (2025).
29. T.D. Le Phuc, B.D. Hardesty, H.J. Auman, A.M. Fischer, Frontal processes as drivers of floating marine debris in coastal areas. Mar. Environ. Res. **200**, 106654 (2024). https://doi.org/10.1016/j.marenvres.2024.106654
30. H. Nakano, M.B. Alfonso, N. Phinchan, S. Jandang, M.R.A. Manap, S. Chavanich, V, Viyakarn, M. Müller, C. Wong, H.P. Bacosa, M. Celik, M.R. Cordova, A. Isobe, Aquatic microplastics research in the ASEAN region: Analysis of challenges and priorities, Mar. Pollut. Bull. **210**, 117342 (2025). https://doi.org/10.1016/j.marpolbul.2024.117342
31. E.A. Kisnarti, S.K.A. Mevia, Macro waste and microplastics on Moyo and Medang Islands, Nusa Tenggara Barat, Indonesia, Microplastics. **4**, 4 **(**2025). https://doi.org/10.3390/microplastics4040102
32. L. Lebreton, J. van der Zwet, J.W. Damsteeg, B. Slat, A. Andrady, J. Reisser, River plastic emissions to the world's oceans. Nat Commun. **8**, 15611 (2017). https://doi.org/10.1038/ncomms15611
33. J. Mansui, A. Molcard, Y. Ourmières, Modelling the transport and accumulation of floating marine debris in the Mediterranean basin. Mar. Pollut. Bull. **91**, 249–257 (2015). https://doi.org/10.1016/j.marpolbul.2014.11.037
34. J.E. Bullard, A. Ockelford, P. O'Brien, C.M. Neuman, Preferential transport of microplastics by wind. Atmospheric Environment. **245**, 118038 (2021). https://doi.org/10.1016/j.atmosenv.2020.118038
35. S. Siregar, L. Yuliadi, N.P. Purba, W. Pranowo, M. Syamsuddin, Pertukaran massa air di Laut Jawa terhadap periodisitas monsun dan Arlindo pada tahun 2015. Depik. **6**(1), 44–59 (2017). https://doi.org/10.13170/depik.6.1.5523